Published in final edited form as:
J Immunol. 2010 September 15; 185(6): 3740–3749. doi:10.4049/jimmunol.1001231.

Activation of macrophages by $P2X_7$-induced microvesicles from myeloid cells is mediated by phospholipids and is partially dependent on TLR4

L. Michael Thomas[*] and **Russell D. Salter**[*]

Russell D. Salter: rds@pitt.edu

[*] Department of Immunology, University of Pittsburgh School of Medicine, Pittsburgh, PA 15261. Phone: 412.648.9471. Fax: 412.383.8096

Abstract

ATP-mediated activation of the purinergic receptor $P2X_7$ elicits morphological changes and pro-inflammatory responses in macrophages. These changes include rapid shedding of microvesicles (MV), and the non-conventional secretion of cytokines, such as IL-1β and IL-18 following priming. Here we demonstrate the activation potential of $P2X_7$-induced MV isolated from non-primed murine macrophages. Co-treatment of non-primed macrophages with ATP and calcium ionophore induced a rapid release of MV that were predominantly 0.5–1 μm in size. Exposure of primary murine bone marrow-derived macrophages to these MV resulted in co-stimulatory receptor upregulation and TNF-α secretion. Cell homogenates or supernatants cleared of MV did not activate macrophages. MV-mediated activation was p38 MAPK and NF-κB-dependent, and partially dependent on TLR4 activity, but was HMGB1 independent. Biochemical fractionation of the MV demonstrated that the phospholipid fraction, not the protein fraction, mediated macrophage activation through a TLR4 dependent process. $P2X_7$ activation is known to induce calcium independent phospholipase A_2 ($iPLA_2$), calcium dependent phospholipase A_2 ($cPLA_2$), and phospholipase D (PLD) activities, but inhibition of these enzymes did not inhibit MV generation or shedding. However, blocking PLD activity resulted in release of MV incapable of activating recipient macrophages. These data demonstrate a novel mechanism of macrophage activation resulting from exposure to MV from non-primed macrophages, and identifies phospholipids in these MV as the biologically active component. We suggest that phospholipids delivered by MV may be mediators of sterile inflammation in a number of diseases.

Introduction

Released microvesicles (MV) mediate intercellular communication between multiple cell types, and affect cytokine secretion, inflammatory processes, and tumor progression (1). MV can be released from intracellular storage sites or shed directly from the cell surface. Release of plasma membrane-derived MV is typically regulated by intracellular Ca^{2+} mediated processes (2,3), or by protein kinase B (4) or protein kinase C (5,6), and may involve engagement of a number of cell type specific receptors. Shedding typically involves a budding process, in which surface blebs selectively accumulate cellular constituents that are then packaged into MV. In contrast, MV deriving from inside cells include secretory lysosomes (7–9), characterized by expression of lysosomal proteases and other markers, and

Address correspondence and reprint requests to Russell D. Salter, Department of Immunology, University of Pittsburgh School of Medicine, E1052 BST, 3550 Terrace St., Pittsburgh, PA 15261. rds@pitt.edu.

Disclosures
The authors have no financial conflict of interest.

exosomes (1,10), which are stored in multivesicular bodies before being released by an active exocytic process.

In macrophages and other myeloid cells, engagement of $P2X_7$ purinergic receptors triggers the release of MV deriving from both inside the cell (8,11,12) and from the plasma membrane (2,3,13–15). Secretion of IL-1β mediated by $P2X_7$ was suggested to occur through the release of cell surface derived MV many years ago (14), but the content of these MV is still unclear. A more recent study suggests that the majority of IL-1β containing MV may be exosomes as opposed to larger shedding vesicles (11). Members of the IL-1 family, including IL-1β, IL-1α, and IL-18, are stored as inactive precursors and their release after processing can be MV-mediated (2,3,11,14) but this does not exclude other mechanisms of secretion (16–18). In any case, rapid secretion of mature IL-1β requires the NLRP3 inflammasome, which recruits caspase-1, allowing cleavage of the pro-form of the cytokine to its bioactive form (19). Some exosomes from macrophages contain Class II MHC and their exocytosis requires the NLRP3 inflammasome despite being caspase-1 independent (12). Less clear is the requirement for NLRP3 in controlling the $P2X_7$-dependent release of secretory lysosomes (8) although their exocytosis from human monocytes is caspase-1 independent.

Macrophages and other cells of the phagocytic lineage bind and internalize MV from various sources with diverse effects on their function (10). Human monocytes binding tumor derived MV become activated, expressing increased HLA-DR, reactive oxygen species, and TNF-α through a CD44-dependent mechanism (20). In another study, human tumor-derived MV promote differentiation of CD14+ myeloid cells, resulting in an HLA-DR low phenotype lacking CD80 and CD86 expression, and secreting TNF-α, TGFβ, and IL-6, with suppressive effects on T cell proliferation (21). Less is known about potential immune stimulatory effects that macrophage-derived $P2X_7$-induced MV may exert, which could involve IL-1β.

To address this question, we induced MV shedding from non-primed mouse primary macrophages or cell lines through $P2X_7$ activation and tested isolated MV for their ability to activate bone marrow derived macrophages (BMDM). We found that MV were able to activate BMDM in a partially TLR4-dependent manner and that the stimulatory component within the MV was found within phospholipid fractions. MV derived phospholipids activated macrophage through TLR4. Furthermore, MV induced activation is independent of observed loaded cargo such as IL-1β, TNF-α, and HMGB1.

Materials and Methods

Cell culture and reagents

J774A.1 (TIB-67™; ATCC; Manassas, VA), a murine macrophage cell line, and D2SC-1, a murine splenic derived immature dendritic cell line (a gift from Lawrence P. Kane, University of Pittsburgh) were maintained in DMEM (Mediatech; Manassas, VA) supplemented with 10% FBS (Gemini Bio-Products; West Sacramento, CA), 1% additional L-glutamine (Lonza; Basel, Switzerland), and 1% penicillin and streptomycin (Lonza) (hereafter called DMEM complete). FSDC, a murine fetal skin derived immature dendritic cell line (a gift from Paola Ricciardi-Castagnoli, Singapore Immunology Network), and THP-1, a human monocyte cell line (ATCC, Rockville, MD), were maintained in IMDM (Lonza) supplemented with 10% FBS, 1% additional L-glutamine, and 1% penicillin and streptomycin (hereafter called IMDM complete). For experiments, THP-1 cells were treated with 20 μM PMA for 2 days to differentiate them to become more macrophage-like. RAW264.7 murine macrophage cell line transfected with NF-κB reporter plasmid pNF-κB-MetLuc Vector (Clontech; Mountain View, CA) encoding inducible *Metridia* luciferase

protein expression and secretion was a gift from Robert J. Binder (University of Pittsburgh) and was maintained in DMEM complete supplemented with 500 μg/ml G418. Murine bone marrow derived macrophages (BMDM) were derived from C57BL/6 bone marrow (gift from Lisa Borghesi, University of Pittsburgh) and were differentiated with L-cell supplemented media as described previously (22). TLR4−/− mouse bone marrow (23) was a gift from Robert M. O'Doherty (University of Pittsburgh). RAGE−/− mouse bone marrow (24) was a gift from Tim D. Oury (University of Pittsburgh). All knock-out mouse bone marrow described were of the C57BL/6 background.

Other reagents include ATP (Thermo Fisher Scientific; Waltham, MA), A23187 (Sigma; St. Louis, MO), A 438079 (Tocris Bioscience; Ellisville, MO), A 740003 (Tocris Bioscience), brefeldin A (Sigma), SB203580 (EMD Chemicals; Gibbstown, NJ), BATPA/AM (EMD Chemicals), Bisindolylmaleimide I HCl (BIM) (EMD Chemicals), MDL-12330A (Enzo Life Sciences; Farmingdale, NY), H-89 2HCl (EMD Chemicals), CAY10593 (Enzo Life Sciences), CAY10594 (Enzo Life Sciences), bromoenol lactone (BEL) (Enzo Life Sciences), LPS from *Escherichia coli* 026:B6 (Sigma), Poly I:C (Sigma), synthetic MPLA (Invivogen; San Diego, CA), LAL QCL-1000 (Lonza; used according to manufacturer's protocol to assess endotoxin levels), and soluble RAGE (24) was a gift from Tim D. Oury.

Yo-Pro-1 uptake by cells

To measure $P2X_7$-induced large pore formation, 1×10^6 J774A.1 were pre-treated with or without 100 μM A 740003 for 15 minutes before exposure to ATP for 30 minutes, and then were stained with 5 μM Yo-Pro-1 (Invitrogen; Carlsbad, CA). Cells were kept on ice until flow cytometric analysis, which was performed with a BD Biosciences LSR II and results analyzed using FlowJo software (Tree Star, Inc.; Ashland, OR).

MV generation and harvest

J774A.1 and other myeloid cell types were plated in T225 cm^2 flasks in duplicate per treatment. Cells were washed twice with PBS before adding inhibitors in serum-free DMEM with no additions. Cells were then treated with 3 mM ATP and 10 μM A23187 in a final volume of 20 ml of serum-free DMEM with no additions for 30 minutes at 37°C. Supernatant was harvested and centrifuged at 309.1 × g for 10 minutes at 4°C to remove cells and larger debris. MV were collected by centrifugation at 100,000 × g ultracentrifugation for one hour at 4°C. The pellet material from the 100,000 × g ultracentrifugation was re-suspended in 500 μl of PBS. MV were disrupted with 10 passes through a 27 gauge needle. Bradford Assay (Thermo Fisher Scientific) was used to determine the protein concentration with each MV fraction according to manufacturer's specifications. MV were either used immediately or stored at −20°C for later use.

For biochemical fractionation of MV, proteins and lipids were separated through the Bligh and Dyer method of protein/lipid extraction with 1:2 of chloroform and methanol (25). The protein fraction was harvested at the biphasic interphase and reconstituted in PBS. The lipid fraction was either dried by speed vacuum centrifugation or further separated through a lipid polarity extraction technique (26). Lipid extract was passed through a silicic acid (Sigma) column (1 mg of silicic acid per 1 μl volume of lipid extract). The pass through was collected as a sample. Bed layer volumes of chloroform, acetone, and then methanol were passed in sequential and separate fashion to elute off potential neutral lipids, glycolipids/ sulpholipids, and phospholipids respectively. Samples were harvested from each elute, dried with speed vacuum centrifugation, and stored at −20°C.

Generating cell homogenate

Ten million J774A.1 were washed twice in PBS, pelleted and resuspended in homogenization buffer (100 mM KCl, 25 mM NaCl, 2 mM $MgSO_4$, 12 mM sodium-citrate, 10 mM glucose, 25 mM HEPES [N-2-hydroxyehylpiperazine-N′-2-ethanesulfonic acid], 5 mM ATP, 0.35% BSA, pH 7.0) supplemented with protease inhibitor cocktail (Sigma). Cells were lysed through 4 cycles of freeze-thawing and homogenized with 30 strokes within a tight-fitting dounce homogenizer. The homogenate was then ultracentrifugated at 100,000 × g for 1 hour at 4°C. Resulting pellets were resuspended in 500 μl of PBS then homogenized with 10 passes through a 27 gauge needle. Samples were used immediately or stored at −20°C.

Measuring activation of treated BMDM

BMDM (WT or knock-out derived where indicated) were harvested following differentiation and plated at 1×10^6 cells/ml in IMDM complete (unless described differently) in petri dishes. Inhibitors where indicated were applied for at least 30 minutes prior to exposure to MV or other compounds, and were maintained throughout the experiment. Supernatants were tested for TNF-α ELISA (eBioscience; San Diego, CA), IL-12p70 ELISA (eBioscience), or IL-23 ELISA (eBioscience) according to manufacturers' protocols.

For flow cytometry studies to determine viability and expression of co-stimulatory receptors, cells were blocked with 1.5% normal goat serum diluted in 0.1% BSA in PBS for 20 minutes then stained with APC anti-CD80 (BD Biosciences; San Jose, CA), PE anti-CD83 (BD Biosciences), FITC anti-CD86 (BD Biosciences), APC anti-CD86 (BD Biosciences), or PE anti-I-A^b (BD Biosciences) antibodies for 40 minutes. Cells were stained with 1 μg/ml DAPI (Sigma) viability dye. Flow cytometry was performed with a BD Biosciences LSR II and results analyzed using FlowJo software. MFI and population percentages of FITC, PE, and/or APC were calculated for DAPI negative cell populations (i.e., living cells), which was over 85% of the total cell population for all results and treatments shown here.

RAW264.7 NF-κB reporter assay

RAW264.7 macrophage stably transfected with pNF-κB-MetLuc Vector (Clontech) under G418 selection were plated as 1×10^6 cells/ml of DMEM complete for each treatment. Supernatant following treatment was centrifuged at 10,000 × g for 10 minutes and was then stored at −20°C until used to assay for luciferase activity according to manufacturer's protocol (Clontech). Luminescence readings from each sample were read with an Orion microplate luminometer (Berthold Detection Systems; Huntsville, AL) in duplicate and the average was taken using Simplicity ver 2.1 software (Berthold Detection Systems). Average readings and standard error of the mean were calculated according to the ratio of fold change over non-treated cells at each respective time point of the time course.

Western blotting

For whole cell culture supernatant studies, 2×10^6 J774A.1 were plated in 1 ml of DMEM complete with or without 1 μg/ml of LPS for 4 hours. Cells were washed once with serum-free DMEM with no additions, and treated with or without 3 mM ATP and 10 μM A23187 for 30 minutes. Supernatants were centrifugated at 10,000 × g for 30 seconds and proteins precipitated through a TCA/cholic acid procedure (22) before loading onto a 9% SDS-PAGE gel. SDS-PAGE and protein transfer to 0.45 μm PVDF transfer membrane were performed as previously described (22).

For Western blot analysis of whole cell lysates for phosphorylated and total p38 expression, 1×10^6 BMDM were plated with or without 1 μg/ml LPS or 25 μg protein equivalents/ml of J774A.1 derived MV for 2, 10, 30, or 60 minutes. Following the time course, cells were washed once with PBS then given 100 μl of 1% Triton X-100 lysis buffer in the presence of protease inhibition cocktail (Sigma) and phosphatase inhibition (Sigma) for 15 minutes on ice. Lysates were collected and centrifuged at 10,000 × g for 10 minutes at 4°C before addition of sample buffer and loading onto 11% SDS-PAGE gels.

Western blot was performed using the SNAP-ID according to manufacturer's procedures (Millipore; Billerica, MA). Antibodies for Western blotting included 0.5 μg/ml of mouse anti-HMGB1 antibody (Abcam; Cambridge, MA), 6 μg/ml of mouse anti-IL-1beta antibody (3ZD; National Cancer Institute Biological Resources Branch; Frederick, MD), 0.1 μg/ml of rabbit anti-phospho-p38 (Thr180/Try182 epitope) (Millipore), 1:2,000 diluted rabbit anti-p38 (Poly6224; BioLegend; San Diego, CA), 1:1,666.7 diluted HRP-conjugated goat anti-mouse IgG (Santa Cruz Biotechnology; Santa Cruz, CA), and 1:1,666.7 diluted HRP-conjugated donkey anti-rabbit IgG (BioLegend). Signals were developed using Western Blotting Luminol Reagent (Santa Cruz Biotechnology). Imaging was performed with KODAK Image Station 4000MM and its accompanying KODAK MI SE Software Informer (Carestream Molecular Imaging; New Haven, CT). In some instances, the membrane was stripped for Western blot re-probing with Restore Western Blot Stripping Buffer (Thermo Fisher Scientific) according to manufacturer's protocols.

Biotinylation and Cy5 labeling of MV and uptake by BMDM

MV were labeled with biotin or Cy5 using EZ-Link Sulfo-NHS-SS-Biotin reagent (Thermo Scientific) or monoreactive Cy5 dye (GE Healthcare; Piscataway, NJ) respectively for 1 hour in the 500 μl PBS reconstitution using the protocols supplied by the manufacturers. An additional wash with PBS followed by ultracentrifugation at 100,000 × g for 1 hour at 4°C was used to remove non-conjugated biotin or Cy5 reagent. Sizing of MV was performed with BD Biosciences FACSAria with various sized YG beads (Polysciences; Warrington, PA).

For assessing MV association with recipient BMDM, 1×10^6 BMDM were plated on 12 mm poly-D-lysine coated coverslips in petri dishes. Cells were allowed to adhere for at least 4 hours. Indicated amounts of Cy5 labeled or biotinylated MV were given to the BMDM for varying times. Cells not associated to the coverslips are harvested and processed for FACS analysis of CD86 and biotin/Cy5 label. For some experiments, coverslip associated cells were further stained with CMFDA as a cytoplasmic counterstain (Invitrogen) and LysoTracker Red to label lysosomal compartments (Invitrogen) according to manufacturer's protocols. Coverslips were then washed, 2% PFA fixed, then permeabilized and blocked with 0.5% saponin, 1.5% normal goat serum, and 1% BSA in PBS for 30 minutes. Alexa647 conjugated streptavidin (Invitrogen) and FITC-anti-CD86 (BD Biosciences) were used at 1:100 dilution for 1 hour to visualize biotin and CD86 expression respectively. After successive washes, the coverslips were stained for nuclei with 1 μg/ml DAPI then mounted with gelvatol. Confocal microscopy images were taken with an Olympus Fluoview 1000 (Inverted) and accompanying software (Olympus America Inc.; Center Valley, PA). Laser excitations and emissions were performed sequentially for DAPI, Cy5/Alexa647, LysoTracker Red, and FITC/CMFDA and background noise was minimized. Differential interference contrast microscopy images for each field of view were also taken. Final images were then directly exported to Adobe Photoshop CS2 (Adobe; San Jose, CA).

Statistical analyses

Unpaired student's T-test or one-way ANOVA analyses were performed using Graph Pad Prism (GraphPad Software; La Jolla, CA). *P* values were calculated where indicated and for all statistical studies $P<0.05$ was considered as significant. Notation within figures include $P<0.05$ (*), $P<0.01$ (**), $P<0.001$ (***) and n.s. for not significant.

Results

ATP-induced MV drive de novo TNF-α secretion and upregulate co-stimulatory receptor surface expression in macrophages

J774A.1, a murine macrophage cell line that expresses $P2X_7$ (27) was used to produce MV in response to 3 mM ATP plus 10 μM A23187. While ATP alone was sufficient for generating detectable levels of MV, the addition of the calcium ionophore A23187 produced greater quantities of MV as judged by Bradford assay of collected material (data not shown). A23187 alone did not induce MV release. These results suggested that MV release is $P2X_7$ dependent, and enhanced by A23187. To test this, J774A.1 cells were treated with $P2X_7$ inhibitors A 740003 or A 438079 prior to generating MV. To confirm that the inhibitors blocked P2X7 activity, we measured Yo-Pro-1 uptake, a common measure of $P2X_7$-induced pore formation (28). While treatment with 3 mM ATP alone was sufficient to induce Yo-Pro-1 uptake, co-treatment with 10 μM A23187 and 3 mM ATP greatly increased the signal (Fig 1*A*). Furthermore, Yo-Pro-1 uptake by cells exposed either to 3 mM ATP or to 3 mM ATP plus 10 μM A23187 was blocked by pre-treatment with A 740003 inhibitor. Both $P2X_7$ inhibitors either completely abolished or significantly decreased MV shedding as determined through protein concentration determination by Bradford Assay (Fig. 1*B*). These results demonstrate that MV shedding induced by ATP is dependent on $P2X_7$ activity, as others have shown (2,3,11,12). MV isolated from culture supernatants by ultracentrifugation were analyzed by flow cytometry and range in size from 0.5–1 μm (Supplemental Fig. 1*A*).

To study the effect of MV on macrophage function, purified MV were incubated with BMDM for 18 hours and supernatants were analyzed by ELISA for TNF-α. MV induced TNF-α secretion in a dose-dependent fashion, with the highest dose of MV (75 μg protein equivalents) stimulating more TNF-α secretion than LPS (Fig. 1*C* and *D*). Importantly, an equivalent amount of cell homogenate from J774A.1 cells did not induce TNF-α secretion at significant levels. MV-depleted ultracentrifugation supernatant from MV generation also did not induce TNF-α at significant levels.

CD86 surface expression was also upregulated in a dose-dependent fashion following exposure to MV (Fig. 1*E*). Importantly, cell homogenates and MV-depleted supernatants did not increase CD86 levels compared to non-treated control BMDM (Fig. 1*E*). To exclude the possibility that CD86 upregulation reflected a passive uptake of the protein from MV, BMDM were pre-treated with brefeldin A (BFA). This significantly diminished CD86 upregulation induced by MV, suggesting that observed increase of CD86 was due to transport of endogenously synthesized CD86 to the cell surface (Fig. 1*F*). Similar results of CD86 upregulation were also observed for BMDM treated with MV generated from BMDM, human monocyte cell line THP-1, the murine splenic dendritic cell line D2SC-1, and the murine fetal skin derived dendritic cell line FSDC (Fig. 1*G*).

Exposure of cells to MV also upregulated the expression of other markers of activation, specifically CD80, CD83, and $I\text{-}A^b$ (Fig. 2*A*). We next characterized the potential for MV to elicit the production of cytokines known to have roles in polarizing Th1 and Th17 responses. In contrast to TNF-α however, no increase in IL-12p70 or IL-23 were observed following treatment (Fig. 2*B*). These data demonstrate that $P2X_7$ -induced MV contain a stimulatory activity that can activate macrophages and is not present in equivalent amounts of

homogenates of the cells from which the MV derive. This also suggests that MV primarily stimulate innate immune responses in myeloid cells as opposed to directly influencing adaptive responses.

MV bind rapidly to BMDM and are largely retained at the plasma membrane before inducing TNF-α secretion and CD86 upregulation

To examine their interaction with BMDM, MV were first biotinylated. After washing and re-pelleting, biotinylated MV were incubated for varying times with BMDM. Alexa647-labeled streptavidin was then added to visualize the interaction. When added to BMDM, MV bound to the cell surface within 30 minutes with little increase seen over time (Fig. 3*A* and *B*). In contrast, CD86 expression increased steadily, reaching an observed maximum at 18 hours. Similar kinetics were seen with TNF-α secretion (Fig. 3*C*). Confocal microscopy demonstrated that CD86 and MV were not co-localized at the cell surface; additionally, by 4 hours some MV congregated within lysosomes while most of the MV remained at the plasma membrane (Supplemental Fig. 2).

MV-induced activation is partially TLR4-dependent and is independent of HMGB1

Damaged cells can release a number of compounds (such as damage associated molecular patterns a.k.a DAMPs) that can activate immune cells through TLR engagement. In particular, HMGB1 (29), hyaluronic acid (30) and S100A8/S100A9 complex (31) amongst others activate TLR4 for cellular activation. To examine whether MV activate through a TLR4-dependent pathway, BMDM were generated from WT and TLR4−/− mice. TNF-α induction by MV was reduced in TLR4−/− BMDM, which produced 35–81% less TNF-α than WT BMDM; however, the decrease was not statistically significant (Fig. 4*A*). TLR4−/− BMDM were significantly impaired in CD86 upregulation when treated with MV compared to WT BMDM (Fig. 4*B*). In contrast, CD86 upregulation induced by the TLR4 agonist MPLA was completely dependent on TLR4, while poly I:C stimulation was shown to be TLR4-independent as expected. These data suggest that MV contain a stimulatory component that activates BMDM via TLR4, but that additional means of activation that are not dependent on TLR4 may also be present.

Given the partial TLR4 response from macrophage derived MV, HMGB1 could mediate MV-induced activation. HMGB1 can activate monocytes and macrophages (32) through TLR2, TLR4, and RAGE (29). Also, HMGB1 can be released from activated monocytes and macrophage (33) or necrotic cells (34) and is expressed within secretory lysosomes that are released from monocytes following stimulation with ATP (35). Furthermore, unlike hyaluronic acid and S100A8/S100A9 complexes, which require prior priming through agents like IFN-γ or LPS (36–38), HMGB1 can be passively released through cellular damage in non-primed cells (39). Indeed, HMGB1 was detected in the supernatants of ATP/A23187 treated J774A.1 cells and also in purified MV, but not in supernatants from untreated or LPS only treated cells (Fig. 5 *A*, *B*). LPS treatment before exposure to ATP/A23187 increased secretion of HMGB1 (Fig. 5*A*).

To assess whether MV induced activation requires RAGE, BMDM from RAGE-deficient mice were generated. We determined that there were no significant differences in TNF-α release between MV treated WT and RAGE−/− BMDM (Fig. 5*C*) following stimulation with either LPS or MV. To determine more broadly whether HMGB1 is a stimulatory agent in MV-induced activation, BMDM were incubated with MV in the presence of soluble RAGE, which through competitive inhibition should block the binding of HMGB1 to all of its potential receptors. Soluble RAGE co-incubated with MV did not diminish MV-mediated TNF-α release (Fig. 5*C*). Additionally, there were no significant differences in CD86 upregulation between WT and RAGE−/− BMDM however, demonstrating that RAGE does

not participate in MV-induced activation (Fig. 5*D*). Furthermore, soluble RAGE did not block MV-induced CD86 upregulation even at high concentrations, suggesting that HMGB1 does not mediate MV activation (Fig. 5*E*).

Characterizing MV-induced signaling pathways

NF-κB and p38 MAPK activation pathways are commonly initiated through TLR engagement (40). Indeed, in BMDM p38 phosphorylation was induced within minutes of exposure to MV, and then declined over time, similar to the response to LPS (Fig. 6*A*). To address whether p38 MAPK blockade was sufficient to diminish MV mediated CD86 upregulation, BMDM were pre-incubated with a titration of the phosphorylated p38 inhibitor SB203580 before exposure to MV. In the presence of the drug, CD86 upregulation was strongly inhibited, supporting a role for p38 MAPK in MV-mediated activation (Fig. 6*B*). In contrast, LPS induced CD86 expression increased in the presence of the 1 μM and 10 μM of the inhibitor with significant inhibition only observed at 50 μM, suggesting differences in the two signaling pathways (data not shown).

We also tested whether MV were able to activate NF-κB, using a RAW264.7 reporter cell line (Fig. 6*C*). The kinetics of the response induced by MV were similar to LPS, with activation evident after 4 and 18 hours but not after 1 hour. The magnitude of the response was less with MV than with LPS however, and declined by 18 hours post-treatment.

PKA and PKC can influence p38 and NF-κB in immune cells (40). PKC is largely modulated with intracellular calcium or diacylglycerol (41) whereas PKA is cAMP controlled (42). To indirectly inhibit PKC, BMDM were treated with 30 μM BAPTA/AM to chelate intracellular calcium. Treatment did not impair CD86 upregulation in response to MV or LPS (Fig. 7*A*). Direct PKC inhibition through use of 50 μM Bisindolylmaleimide I HCl (BIM) significantly decreased MV mediated CD86 upregulation (Fig. 7*B*). In contrast, PKC inhibition enhanced LPS mediated CD86 upregulation. MDL-12330A was used to inhibit adenylate cyclase, which generates cAMP, resulting in a significant decrease in expression from MV but not LPS treated BMDM (Fig. 7*C*). Inhibition of PKA using 10 μM H-89 HCl also resulted in a significant decrease (Fig. 7*D*). These results support that MV mediated activation requires PKA and PKC pathways, which is in contrast to the observed activation response induced by LPS.

The stimulatory agent from MV consists of one or more phospholipids

To characterize the stimulatory agent(s) from MV, biochemical fractionation was used to separate lipids and proteins as described in Methods. Only the lipid fraction, not protein, significantly activated BMDM, as measured by CD86 upregulation (Fig. 8*A*). Lipids were further separated according to polarity. The phospholipids fraction provided significant upregulation of CD86 as compared to non-treated control. Only minimal activity was recovered from the flow through, the neutral lipids fraction, or the glycolipid/sulpholipid fraction (Fig. 8*B*). Mock elution from the column for a phospholipid fraction also did not recover any stimulatory material, demonstrating that the columns themselves did not contain contaminants that could activate BMDM.

To test the TLR4 dependence of the phospholipid containing fraction from the MV, TLR4−/− or WT BMDM were given equal amounts of phospholipid fraction. In agreement with the partial TLR4 dependence for MV mediated activation as observed in Figure 4, the phospholipid fraction from MV had a significant difference in activation between the TLR4−/− and WT BMDM. Additionally, phospholipid fraction activation of TLR4−/− BMDM did not significantly differ from non-treated BMDM. This would at least partially confirm that the TLR4 agonist from the MV came in the form of a phospholipid.

Lipid modifying enzymes play a role in generating MV capable of activating BMDM

These results led us to hypothesize that purinergic receptor activation in MV producer cells exposed to ATP might generate stimulatory phospholipids that are packaged into MV. This could explain why MV activated BMDM more strongly than the equivalent amount of cell lysate, as described earlier. $P2X_7$ activation, which is required for generating ATP-induced MV, can activate lipid modifying enzymes such as $iPLA_2$ (43), PLD (44), and $cPLA_2$ (43). To test whether PLD, $iPLA_2$, or $cPLA_2$ were required in generating stimulatory MV, producer cells were treated with either PLD inhibitors (50 μM CAY10593 for PLD1 and 50 μM CAY10594 for PLD2), $iPLA_2$ inhibitor bromoenol lactone (10 μM BEL), or $cPLA_2$ inhibitor (10 μM AACOF3) 30 minutes prior to and during 3 mM ATP and 10 μM A23187 administration for MV induction. When equivalent amounts of these respective MV populations were applied to recipient BMDM, MV from PLD1 and PLD2-inhibited J774A.1 producer cells were unable to stimulate CD86 upregulation (Fig. 9*A*). PLD inhibitors used to inhibit PLD during MV generation did not directly impact MV-mediated CD86 upregulation of recipient BMDM as inclusion of MV from PLD1 and PLD2-inhibited J774A.1 with MV from mock treated J774A.1 did not result in any significant differences from BMDM treatment with MV from mock treated J774A.1 (Fig. 9*B*). Furthermore, MV from mock treated or from PLD1 or PLD2 inhibited cells did not decrease phosphatidic acid levels of treated J774A.1 recipient cells relative to non-treated J774A.1 (data not shown). In contrast to PLD, inhibition of $iPLA_2$ (Fig. 9*C*) or $cPLA_2$ (Fig. 9*D*) in MV producer cells did not decrease the stimulatory capacity of the MV generated, which were at least as potent as those from producer cells not pretreated with inhibitors. It should be noted that MV were obtained from producer cells treated with these inhibitors in amounts roughly equal to mock-treated producer cells, suggesting that the stimulatory phospholipid is not required for MV structural integrity or secretion from cells. Furthermore, PLD1, PLD2, $iPLA_2$, and $cPLA_2$ inhibitors were not toxic at the tried concentrations; cell viability was over 85% (data not shown).

We lastly considered whether lysophosphatidic acid (LPA) could be identified as a potential stimulatory phospholipid from the MV. LPA is a product of $P2X_7$ activity (45) and it can activate macrophages to promote cytokine production (46) and cAMP synthesis (47). Pre-treatment of BMDM with Ki16425, a lysophosphatidic acid receptor inhibitor selective for LPA_1 and LPA_3 receptors did not diminish CD86 upregulation by MV (Fig. 9*E*). This suggests LPA does not participate in MV-induced activation of macrophages, although it does not exclude the possibility that LPA could mediate effects through other receptors.

Discussion

MV released by cells can potently influence immune responses in a number of ways. Many cell types release exosomes constitutively, and, depending on the cell of origin, may transfer antigens or other cargo to DC that can initiate immune responses. A specialized type of MV release exists for myeloid cells that express $P2X_7$ receptors, which, when exposed to receptor agonists such as ATP, shed MV from the cell surface as well as release them from intracellular stores. Characterizing MV generation induced by $P2X_7$ activation on macrophages is important for understanding inflammatory processes, since tissue damage has been shown to release intracellular constituents like ATP into an environment containing large numbers of these cells (48–51).

When macrophages are primed by exposure to TLR agonists, cytokines including IL-1β and TNF-α, are synthesized and may be released from the cell following appropriate stimulation by a secondary signal (19). For IL-1β release, $P2X_7$ engagement is followed by cleavage of pro-IL-1β into the bioactive form by caspase-1 in a NLRP3-dependent process. MV have been demonstrated to contain mature IL-1β and were first characterized as surface derived

vesicles (3,14), but later as exosomes (11). TNF-α-containing exosomes have been reported to be secreted from human melanoma cells (52). We have detected TNF-α within $P2X_7$-induced MV from primed macrophages; however, TNF-α was also detected from cell-culture supernatants devoid of MV (data not shown). Nevertheless, only primed macrophages would release pro-inflammatory cytokines, whose synthesis primarily depends on NF-κB activation (40), whether in MV or as a soluble proteins.

Our study instead focuses on characterizing the biological effects of MV released by non-primed, primary macrophages, a condition which may be seen during sterile inflammation. As reported by others, MV are released following $P2X_7$ engagement in non-primed macrophages (12), yet to the best of our knowledge, have not been studied for their ability to activate macrophages. While 3 mM ATP alone is sufficient for $P2X_7$ activation, we observe enhanced $P2X_7$ activity when co-administering 10 μM A23187 with 3 mM ATP. A23187 with 0.3 mM ATP was not able to induce $P2X_7$ activity; thus in this manner, A23187 is serving in some other function than for the autocrine release of endogenously stored ATP for $P2X_7$ activation. We found that $P2X_7$-induced MV from non-primed myeloid cells can induce expression of CD86, CD80, CD83, and Class II MHC (Fig. 2*A*), and also induce secretion of TNF-α from primary macrophages (Fig. 1*A*, *B*). We further characterized the contents of these MV and found that phospholipids were responsible for stimulating macrophage activation in a TLR4-dependent process (Fig. 8*B*). As separated phospholipids from MV activate macrophages, we can exclude a requirement for interaction of intact MV in this process. That being said, based on our observation that MV mediated activation was only partially TLR4-dependent, we hypothesize that MV must contain components in addition to phospholipids that activate macrophages independently of TLR4 and that these activities may be contingent upon intact MV delivery into intracellular departments.

Stimulation of primed macrophages by $P2X_7$ yields MV that are heterogeneous, consisting of exosomes (11,12) and surface-derived vesicles (3,14), and possibly including secreted lysosomes (7–9). The MV described in our study are predominantly 0.5–1.0 μm in diameter (Supplemental Fig. 1*A*), distinguishing them from larger 1–4 μm apoptotic blebs (53). We observed relatively few smaller MV that would be characteristic of exosomes as analyzed by EM (data not shown), and believe that our preparations were devoid of them for several reasons. While our MV were obtained from ultra-centrifugation at 100,000 × g, we also found that material obtained from 10,000 × g centrifugation exert equivalent ability to activate macrophage (data not shown). Exosomes do not pellet at the low speed as they are only 50–100 nm in diameter. Thus, MV-induced macrophage activation seems to be exosome independent. Furthermore, the release of Class II MHC containing exosomes from macrophages requires ASC/NLRP3 inflammasome (12). Non-primed myeloid cells, such as we have used, typically do not express high levels of NLRP3 (54), and thus would not be expected to release Class II MHC+ exosomes efficiently. In addition, we have purified MV from D2SC-1 cells, a murine splenic DC-derived cell line that lacks ASC (data not shown), and found that these MV are potent stimulators of macrophage activation (Fig. 1*G*). In this way, D2SC-1 act similarly to RAW264.7, which also lack ASC (27) yet also shed MV in response to $P2X_7$ stimulation (55). These results support the conclusion that MV distinct from previously characterized Class II MHC+ exosomes are shed by myeloid cells and stimulate primary macrophages through a TLR4-dependent process involving recognition of phospholipids contained within MV.

Endogenous phospholipids can activate macrophage through TLR4 activities. Recently, it was demonstrated that oxidized low density lipoprotein (oxLDL), which bind to the scavenger receptor B family member CD36, can promote sterile inflammation through activation of TLR4/6 heterodimer on macrophages (56). Both cell death (57,58) and foam-cell formation (59) have also been shown to be induced by oxidized LDL through TLR4 in

macrophages. Furthermore, oxidized phospholipids from minimally modified low density lipoprotein (mmLDL), which contain essentially the same phospholipids as oxLDL, stimulate macrophage ROS generation (60), ERK activation (61), membrane spreading (62), and inhibition of phagocytic uptake of apoptotic bodies (62), through a partially TLR4-dependent pathway. Whether phospholipids in $P2X_7$-induced MV are structurally similar to those in oxLDL or mmLDL will be addressed in future studies. Our study suggests that the stimulatory phospholipid is not lysophosphatidic acid (Fig. 9*E*). We were also unable to induce BMDM activation with commercially available lysophosphatidic acid, phosphatidic acid, or phosphatidylserine (data not shown).

Importantly, $P2X_7$-induced MV from PLD1- and PLD2- inhibited MV producer cells were unable to activate macrophages (Fig. 9*A*); at the same time, MV yields were equivalent between drug treated and non-drug treated cells (data not shown). This dissociates MV formation from incorporation of the stimulatory phospholipid into vesicles, and suggests that generation of a bioactive phospholipid results from $P2X_7$ activation leading to downstream PLD activation. While PLD (44) and $iPLA_2$ (43) are activated following $P2X_7$ activation (data not shown), blocking PLD activity but not $iPLA_2$ impaired the MV activating capacity (Fig. 9). These results may explain why cell homogenates of producer cells were unable to stimulate macrophage activation (Fig. 1*B, C*), since PLD was not activated. Activated PLD produces phosphatidic acid (PA) to coordinate ADP-ribosylation factor-6 (ARF-6), a known regulator of exocytosis, to sites of potential exocytosis (63). Future studies will be done to understand the specific PLD activities that enable stimulatory phospholipid loading into $P2X_7$-induced MV.

It has been suggested that host cell derived stimulators of TLR activity might contain microbial contaminants introduced during biochemical purification, a hypothesis described in detail recently in a thought provoking review (64). Based on this, we considered whether MV preparations might contain endotoxin. When tested by LAL assay, endotoxin was present within stimulatory MV preparations at low levels, typically around 0.25 EU/ml (data not shown). However, the same amount of endotoxin is observed in non-stimulatory MV from PLD-inhibited cells (data not shown), indicating that these low levels cannot explain the stimulation we observe. Furthermore, treatment of BMDM with equivalent amounts of LPS to that found in MV (approximately 50 pg/ml of LPS for 25 μg of protein equivalents of MV) did not induce significant TNF-α release or CD86 upregulation (data not shown). It should also be noted that in addition to testing non-stimulatory MV, we observed that cell homogenates and ultracentrifugation supernatants were also devoid of BMDM-stimulating activity.

Our study suggests that MV derived from macrophages in an environment where there is tissue damage without infection could have potent biological activities that may further drive inflammation. In tumors and other settings with significant necrosis, infiltrating macrophages expressing $P2X_7$ would be exposed to elevated levels of extracellular ATP, as previously shown in tumors (65–67). Macrophage-produced MV would then bind to adjacent cells, including macrophages and DC, leading to their activation and resulting in secretion of TNF-α and potentially other pro-inflammatory mediators. The most novel aspect of this work, implicating phospholipids from MV as the stimulatory component, may be consistent with recent work implicating phospholipids in inflammation present in atherosclerotic lesions as discussed above. In cancer and in atherosclerosis, as well as potentially in other pathological settings, there are strong indications that sterile inflammation plays a role in disease processes through largely unknown mechanisms. Innate responses by macrophages in inflammatory diseases may in part be explained by release of stimulatory phospholipids in MV at sites of tissue damage.

Supplementary Material

Refer to Web version on PubMed Central for supplementary material.

Acknowledgments

We are grateful to numerous labs for reagents and bone marrow where indicated, BD Biosciences FACS Aria help from Dewayne H. Falkner (University of Pittsburgh), and for luminometer assistance from Judong Lee from Lawrence P. Kane's lab (University of Pittsburgh) and Sudesh Pawaria from Robert J. Binder's lab. We are also appreciate helpful discussions and cell culture assistance from Michelle E. Heid, Jessica Chu, Peter A. Keyel, and Chengqun Sun from our lab and discussions and reagents from Judson M. Englert from Tim D. Oury's lab. We thank Laura E. Kropp for her critical reading of the manuscript.

This work was supported by the NIH grants R01AI072083 (RDS), P01CA073743 (RDS), and T32CA082084 (LMT).

Abbreviations used in this paper

NLRP3	Nod-like receptor family, pyrin domain containing 3
PLD	phospholipase D
iPLA$_2$	calcium independent phospholipase A$_2$
cPLA$_2$	calcium dependent phospholipase A$_2$
BMDM	bone marrow derived macrophage
PKA	protein kinase A
PKC	protein kinase C
MPLA	monophosphoryl lipid A
HMGB1	high-mobility group box 1
RAGE	receptors for advanced glycation end products
sRAGE	soluble receptors for advanced glycation end products
MV	microvesicles
WT	wild-type
NT	no treatment
MFI	mean fluorescent intensity
LPA	lysophosphatidic acid

References

1. Cocucci E, Racchetti G, Meldolesi J. Shedding microvesicles: artefacts no more. Trends Cell Biol. 2009; 19:43–51. [PubMed: 19144520]
2. Bianco F, Pravettoni E, Colombo A, Schenk U, Möller T, Matteoli M, Verderio C. Astrocyte-derived ATP induces vesicle shedding and IL-1 beta release from microglia. J Immunol. 2005; 174:7268–7277. [PubMed: 15905573]
3. Pizzirani C, Ferrari D, Chiozzi P, Adinolfi E, Sandonà D, Savaglio E, Di Virgilio F. Stimulation of P2 receptors causes release of IL-1beta loaded microvesicles from human dendritic cells. Blood. 2007; 109:3856–3864. [PubMed: 17192399]
4. Baj-Krzyworzeka M, Szatanek R, Weglarczyk K, Baran J, Urbanowicz B, Brański P, Ratajczak MZ, Zembala M. Tumour-derived microvesicles carry several surface determinants and mRNA of tumour cells and transfer some of these determinants to monocytes. Cancer Immunol Immunother. 2006; 55:808–818. [PubMed: 16283305]

5. Pilzer D, Fishelson Z. Mortalin/GRP75 promotes release of membrane vesicles from immune attacked cells and protection from complement-mediated lysis. Int Immunol. 2005; 17:1239–1248. [PubMed: 16091382]
6. Sidhu SS, Mengistab AT, Tauscher AN, LaVail J, Basbaum C. The microvesicle as a vehicle for EMMPRIN in tumor stromal interactions. Oncogene. 2004; 23:956–963. [PubMed: 14749763]
7. Andrei C, Dazzi C, Lotti L, Torrisi MR, Chimini G, Rubartelli A. The secretory route of the leaderless protein interleukin 1beta involves exocytosis of endolysosome-related vesicles. Mol Biol Cell. 1999; 10:1463–1475. [PubMed: 10233156]
8. Andrei C, Margiocco P, Poggi A, Lotti LV, Torrisi MR, Rubartelli A. Phospholipases C and A2 control lysosome-mediated IL-1 β secretion: Implications for inflammatory processes. Proc Natl Acad Sci USA. 2004; 101:9745–9750. [PubMed: 15192144]
9. Gardella S, Andrei C, Lotti LV, Poggi A, Torrisi MR, Zocchi MR, Rubartelli A. CD8(+) T lymphocytes induce polarized exocytosis of secretory lysosomes by dendritic cells with release of interleukin-1beta and cathepsin D. Blood. 2001; 98:2152–2159. [PubMed: 11568002]
10. Théry C, Ostrowski M, Segura E. Membrane vesicles as conveyors of immune responses. Nat Rev Immunol. 2009; 9:581–593. [PubMed: 19498381]
11. Qu Y, Franchi L, Nunez G, Dubyak GR. Nonclassical IL-1 beta secretion stimulated by P2X7 receptors is dependent on inflammasome activation and correlated with exosome release in murine macrophages. J Immunol. 2007; 179:1913–1925. [PubMed: 17641058]
12. Qu Y, Ramachandra L, Mohr S, Franchi L, Harding CV, Nunez G, Dubyak GR. P2X7 receptor-stimulated secretion of MHC class II-containing exosomes requires the ASC/NLRP3 inflammasome but is independent of caspase-1. J Immunol. 2009; 182:5052–5062. [PubMed: 19342685]
13. Baroni M, Pizzirani C, Pinotti M, Ferrari D, Adinolfi E, Calzavarini S, Caruso P, Bernardi F, Di Virgilio F. Stimulation of P2 (P2X7) receptors in human dendritic cells induces the release of tissue factor-bearing microparticles. FASEB J. 2007; 21:1926–1933. [PubMed: 17314141]
14. MacKenzie A, Wilson HL, Kiss-Toth E, Dower SK, North RA, Surprenant A. Rapid secretion of interleukin-1beta by microvesicle shedding. Immunity. 2001; 15:825–835. [PubMed: 11728343]
15. Wilson HL, Francis SE, Dower SK, Crossman DC. Secretion of intracellular IL-1 receptor antagonist (type 1) is dependent on P2X7 receptor activation. J Immunol. 2004; 173:1202–1208. [PubMed: 15240711]
16. Brough D, Rothwell NJ. Caspase-1-dependent processing of pro-interleukin-1beta is cytosolic and precedes cell death. J Cell Sci. 2007; 120:772–781. [PubMed: 17284521]
17. Hogquist KA, Unanue ER, Chaplin DD. Release of IL-1 from mononuclear phagocytes. J Immunol. 1991; 147:2181–2186. [PubMed: 1918954]
18. Singer II, Scott S, Chin J, Bayne EK, Limjuco G, Wiedner J, Miller DK, Chapman K, Kostura MJ. The interleukin-1 beta-converting enzyme (ICE) is localized on the external cell surface membranes and in the cytoplasmic ground substance of human monocytes by immuno-electron microscopy. J Exp Med. 1995; 182:1447–1459. [PubMed: 7595215]
19. Martinon F, Mayor A, Tschopp J. The inflammasomes: guardians of the body. Annu Rev Immunol. 2009; 27:229–265. [PubMed: 19302040]
20. Baj-Krzyworzeka M, Szatanek R, Weglarczyk K, Baran J, Zembala M. Tumour-derived microvesicles modulate biological activity of human monocytes. Immunol Lett. 2007; 113:76–82. [PubMed: 17825925]
21. Valenti R, Huber V, Filipazzi P, Pilla L, Sovena G, Villa A, Corbelli A, Fais S, Parmiani G, Rivoltini L. Human tumor-released microvesicles promote the differentiation of myeloid cells with transforming growth factor-beta-mediated suppressive activity on T lymphocytes. Cancer Res. 2006; 66:9290–9298. [PubMed: 16982774]
22. Chu J, Thomas LM, Watkins SC, Franchi L, Núñez G, Salter RD. Cholersterol-dependent cytolysins induce rapid release of mature IL-1beta from murine macrophages in a NLRP3 inflammasome and cathepsin B-dependent manner. J Leukoc Biol. 2009; 86:1227–1238. [PubMed: 19675207]
23. Radin MS, Sinha S, Bhatt BA, Dedousis N, O'Doherty RM. Inhibition or deletion of the lipopolysaccharide receptor Toll-like receptor-4 confers partial protection against lipid-induced

insulin resistance in rodent skeletal muscle. Diabetologia. 2008; 51:336–346. [PubMed: 18060381]

24. Englert JM, Hanford LE, Kaminski N, Tobolewski JM, Tan RJ, Fattman CL, Ramsgaard L, Richards TJ, Loutaev I, Nawroth PP, Kasper M, Bierhaus A, Oury TD. A role for the receptor for advanced glycation end products in idiopathic pulmonary fibrosis. Am J Pathol. 2008; 172:583–591. [PubMed: 18245812]
25. Bligh EG, Dyer WJ. A rapid method of total lipid extraction and purification. Can J Biochem Physiol. 1959; 37:911–917. [PubMed: 13671378]
26. Christie WW. A simple procedure for rapid transmethylation of glycerolipids and cholesteryl esters. J Lipid Res. 1982; 23:1072–1075. [PubMed: 6897259]
27. Pelegrin P, Barroso-Gutierrez C, Surprenant A. P2X7 receptor differentially couples to distinct release pathways for IL-1beta in mouse macrophage. J Immunol. 2008; 180:7147–7157. [PubMed: 18490713]
28. Donnelly-Roberts D, Namovic M, Han P, Jarvis M. Mammalian P2X7 receptor pharmacology: comparison of recombinant mouse, rat and human P2X7 receptors. Br J Pharmacol. 2009; 157:1203–1214. [PubMed: 19558545]
29. Park JS, Svetkauskaite D, He Q, Kim JY, Strassheim D, Ishizaka A, Abraham E. Involvement of toll-like receptors 2 and 4 in cellular activation by high mobility group box 1 protein. J Biol Chem. 2004; 279:7370–7377. [PubMed: 14660645]
30. Termeer C, Benedix F, Sleeman J, Fieber C, Voith U, Ahrens T, Miyake K, Freudenberg M, Galanos C, Simon JC. Oligosaccharides of Hyaluronan activate dendritic cells via toll-like receptor 4. J Exp Med. 2002; 195:99–111. [PubMed: 11781369]
31. Vogl T, Tenbrock K, Ludwig S, Leukert N, Ehrhardt C, van Zoelen MA, Nacken W, Foell D, van der Poll T, Sorg C, Roth J. Mrp8 and Mrp14 are endogenous activators of Toll-like receptor 4, promoting lethal, endotoxin-induced shock. Nat Med. 2007; 13:1042–1049. [PubMed: 17767165]
32. Andersson U, Wang H, Palmblad K, Aveberger AC, Bloom O, Erlandsson-Harris H, Janson A, Kokkola R, Zhang M, Yang H, Tracey KJ. High mobility group 1 protein (HMG-1) stimulates proinflammatory cytokine synthesis in human monocytes. J Exp Med. 2000; 192:565–570. [PubMed: 10952726]
33. Wang H, Bloom O, Zhang M, Vishnubhakat JM, Ombrellino M, Che J, Frazier A, Yang H, Ivanova S, Borovikova L, Manogue KR, Faist E, Abraham E, Andersson J, Andersson U, Molina PE, Abumrad NN, Sama A, Tracey KJ. HMG-1 as a late mediator of endotoxin lethality in mice. Science. 1999; 285:248–251. [PubMed: 10398600]
34. Scaffidi P, Misteli T, Bianchi ME. Release of chromatin protein HMGB1 by necrotic cells triggers inflammation. Nature. 2002; 418:191–195. [PubMed: 12110890]
35. Gardella S, Andrei C, Ferrera D, Lotti LV, Torrisi MR, Bianchi ME, Rubartelli A. The nuclear protein HMGB1 is secreted by monocytes via a non-classical, vesicle-mediated secretory pathway. EMBO Rep. 2002; 3:995–1001. [PubMed: 12231511]
36. Hu SP, Harrison C, Xu K, Cornish CJ, Geczy CL. Induction of the chemotactic S100 protein, CP-10, in monocyte/macrophages by lipopolysaccharide. Blood. 1996; 87:3919–3928. [PubMed: 8611721]
37. Xu K, Geczy CL. IFN-gamma and TNF regulate macrophage expression of the chemotactic S100 protein S100A8. J Immunol. 2000; 164:4916–4923. [PubMed: 10779802]
38. Zheng L, Riehl TE, Stenson WF. Regulation of colonic epithelial repair in mice by Toll-like receptors and hyaluronic acid. Gastroenterology. 2009; 137:2041–2051. [PubMed: 19732774]
39. Lotze MT, Tracey KJ. High-mobility group box 1 protein (HMGB1): nuclear weapon in the immune arsenal. Nat Rev Immunol. 2005; 5:331–342. [PubMed: 15803152]
40. Akira S, Takeda K. Toll-like receptor signaling. Nat Rev Immunol. 2004; 4:499–511. [PubMed: 15229469]
41. Steinberg SF. Structural basis of protein kinase C isoform function. Physiol Rev. 2008; 88:1341–1378. [PubMed: 18923184]
42. Taylor SS, Yang J, Wu J, Haste NM, Radzio-Andzelm E, Anand G. PKA: a portrait of protein kinase dynamics. Biochim Biophys Acta. 2004; 1679:259–269. [PubMed: 15023366]

43. Alzola E, Peréz-Etxebarria A, Kabré E, Fogarty DJ, Métioui M, Chaïb N, Macarulla JM, Matute C, Dehaye JP, Marino A. Activation by P2X7 agonists of two phospholipases A2 (PLA2) in ductal cells of rat submandibular gland. Coupling of the calcium-independent PLA2 with kallikrein secretion. J Biol Chem. 1998; 273:30208–30217. [PubMed: 9804778]
44. Humphreys BD, Dubyak GR. Induction of the P2z/P2X7 nucleotide receptor and associated phospholipase D activity by lipopolysaccharide and IFN-gamma in the human THP-1 monocytic cell line. J Immunol. 1996; 157:5627–5637. [PubMed: 8955215]
45. Panupinthu N, Zhao L, Possmayer F, Ke HZ, Sims SM, Dixon SJ. P2X7 nucleotide receptors mediate blebbing in osteoblasts through a pathway involving lysophosphatidic acid. J Biol Chem. 2007; 282:3403–3412. [PubMed: 17135244]
46. Lee H, Liao JJ, Graeler M, Huang MC, Goetzl EJ. Lysophospholipid regulation of mononuclear phagocytes. Biochim Biophys Acta. 2002; 1582:175–177. [PubMed: 12069826]
47. Lin WW, Chang SH, Wang SM. Roles of atypical protein kinase C in lysophosphatidic acid-induced type II adenylyl cyclase activation in RAW 264.7 macrophages. Br J Pharmacol. 1999; 128:1189–1198. [PubMed: 10578131]
48. Domercq M, Perez-Samartin A, Aparicio D, Alberdi E, Pampliega O, Matute C. P2X7 receptors mediate ischemic damage to oligodendrocytes. Glia. 2010; 58:730–740. [PubMed: 20029962]
49. Idzko M, Hammad H, van Nimwegen M, Kool M, Willart MA, Muskens F, Hoogsteden HC, Luttmann W, Ferrari D, Di Virgilio F, Virchow JC Jr, Lambrecht BN. Extracellular ATP triggers and maintains asthmatic airway inflammation by activating dendritic cells. Nat Med. 2007; 13:913–919. [PubMed: 17632526]
50. Mortaz E, Braber S, Nazary M, Givi ME, Nijkamp FP, Folkerts G. ATP in the pathogenesis of lung emphysema. Eur J Pharmacol. 2009; 619:92–96. [PubMed: 19654006]
51. Peng W, Cotrina ML, Han X, Yu H, Bekar L, Blum L, Takano T, Tian GF, Goldman SA, Nedergaard M. Systemic administration of an antagonist of the ATP-sensitive receptor P2X7 improves recovery after spinal cord injury. Proc Natl Acad Sci USA. 2009; 106:12489–12493. [PubMed: 19666625]
52. Söderberg A, Barral AM, Söderström M, Sander B, Rosén A. Redox-signaling transmitted in trans to neighboring cells by melanoma-derived TNF-containing exosomes. Free Radic Biol Med. 2007; 43:90–99. [PubMed: 17561097]
53. Qu Y, Dubyak GR. P2X7 receptors regulate multiple types of membrane trafficking responses and non-classical secretion pathways. Purinergic Signal. 2009; 5:163–173. [PubMed: 19189228]
54. Bauernfeind FG, Horvath G, Stutz A, Alnemri ES, MacDonald K, Speert D, Fernandes-Alnemri T, Wu J, Monks BG, Fitzgerald KA, Hornung V, Latz E. Cutting edge: NF-kappaB activating pattern recognition and cytokine receptors license NLRP3 inflammasome activation by regulating NLRP3 expression. J Immunol. 2009; 183:787–791. [PubMed: 19570822]
55. Moore SF, MacKenzie AB. Murine macrophage P2X7 receptors support rapid prothrombotic responses. Cell Signal. 2007; 19:855–866. [PubMed: 17175137]
56. Stewart CR, Stuart LM, Wilkinson K, van Gils JM, Deng J, Halle A, Rayner KJ, Boyer L, Zhong R, Frazier WA, Lacy-Hulbert A, Khoury JE, Golenbock DT, Moore KJ. CD36 ligands promote sterile inflammation through assembly of a Toll-like receptor 4 and 6 heterodimer. Nat Immunol. 2010; 11:155–161. [PubMed: 20037584]
57. Nowicki M, Müller K, Serke H, Kosacka J, Vilser C, Ricken A, Spanel-Borowski K. Oxidized low-density lipoprotein (oxLDL)-induced cell death in dorsal root ganglion cell cultures depends not on the lectin-like oxLDL receptor-1 but on the toll-like receptor-4. J Neurosci Res. 2010; 88:403–412. [PubMed: 19705455]
58. Serke H, Vilser C, Nowicki M, Hmeidan FA, Blumenauer V, Hummitzsch K, Lösche A, Spanel-Borowski K. Granulosa cell subtypes respond by autophagy or cell death to oxLDL-dependent activation of the oxidized lipoprotein receptor 1 and toll-like 4 receptor. Autophagy. 2009; 5:991–1003. [PubMed: 19730000]
59. Chen S, Sorrentino R, Shimada K, Bulut Y, Doherty TM, Crother TR, Arditi M. Chlamydia pneumoniae-induced foam cell formation requires MyD88-dependent and -independent signaling and is reciprocally modulated by liver X receptor activation. J Immunol. 2008; 181:7186–7193. [PubMed: 18981140]

60. Bae YS, Lee JH, Choi SH, Kim S, Almazan F, Witztum JL, Miller YI. Macrophages generate reactive oxygen species in response to minimally oxidized low-density lipoprotein: toll-like receptor 4- and spleen tyrosine kinase-dependent activation of NADPH oxidase 2. Circ Res. 2009; 104:210–218. [PubMed: 19096031]

61. Miller YI, Viriyakosol S, Worrall DS, Boullier A, Butler S, Witztum JL. Toll-like receptor 4-dependent and -independent cytokine secretion induced by minimally oxidized low-density lipoprotein in macrophages. Arterioscler Thromb Vasc Biol. 2005; 25:1213–1219. [PubMed: 15718493]

62. Miller YI, Viriyakosol S, Binder CJ, Feramisco JR, Kirkland TN, Witztum JL. Minimally modified LDL binds to CD14, induces macrophage spreading via TLR4/MD-2, and inhibits phagocytosis of apoptotic cells. J Biol Chem. 2003; 278:1561–1568. [PubMed: 12424240]

63. Zeniou-Meyer M, Zabari N, Ashery U, Chasserot-Golaz S, Haeberle AM, Demais V, Bailly Y, Gottfried I, Nakanishi H, Neiman AM, Du G, Frohman MA, Bader MF, Vitale N. Phospholipase D1 production of phosphatidic acid at the plasma membrane promotes exocytosis of large dense-core granules at a late stage. J Biol Chem. 2007; 282:21746–21757. [PubMed: 17540765]

64. Erridge C. Endogenous ligands of TLR2 and TLR4: agonists or assistants? J Leukoc Biol. 2010; 87:989–999. [PubMed: 20179153]

65. Aymeric L, Apetoh L, Ghiringhelli F, Tesniere A, Martins I, Kroemer G, Smyth MJ, Zitvogel L. Tumor cell death and ATP release prime dendritic cells and efficient anticancer immunity. Cancer Res. 2010; 70:855–858. [PubMed: 20086177]

66. Ghiringhelli F, Apetoh L, Tesniere A, Aymeric L, Ma Y, Ortiz C, Vermaelen K, Panaretakis T, Mignot G, Ullrich E, Perfettini JL, Schlemmer F, Tasdemir E, Uhl M, Génin P, Civas A, Ryffel B, Kanellopoulous J, Tschopp J, André F, Lidereau R, McLaughlin NM, Haynes NM, Smyth MJ, Kroemer G, Zitvogel L. Activation of the NLRP3 inflammasome in dendritic cells induces IL-1beta dependent adaptive immunity against tumors. Nat Med. 2009; 15:1170–1178. [PubMed: 19767732]

67. Martins I, Tesniere A, Kepp O, Michaud M, Schlemmer F, Senovilla L, Séror C, Métivier D, Perfettini JL, Zitvogel L, Kroemer G. Chemotherapy induces ATP release from tumor cells. Cell Cycle. 2009; 8:3723–3728. [PubMed: 19855167]

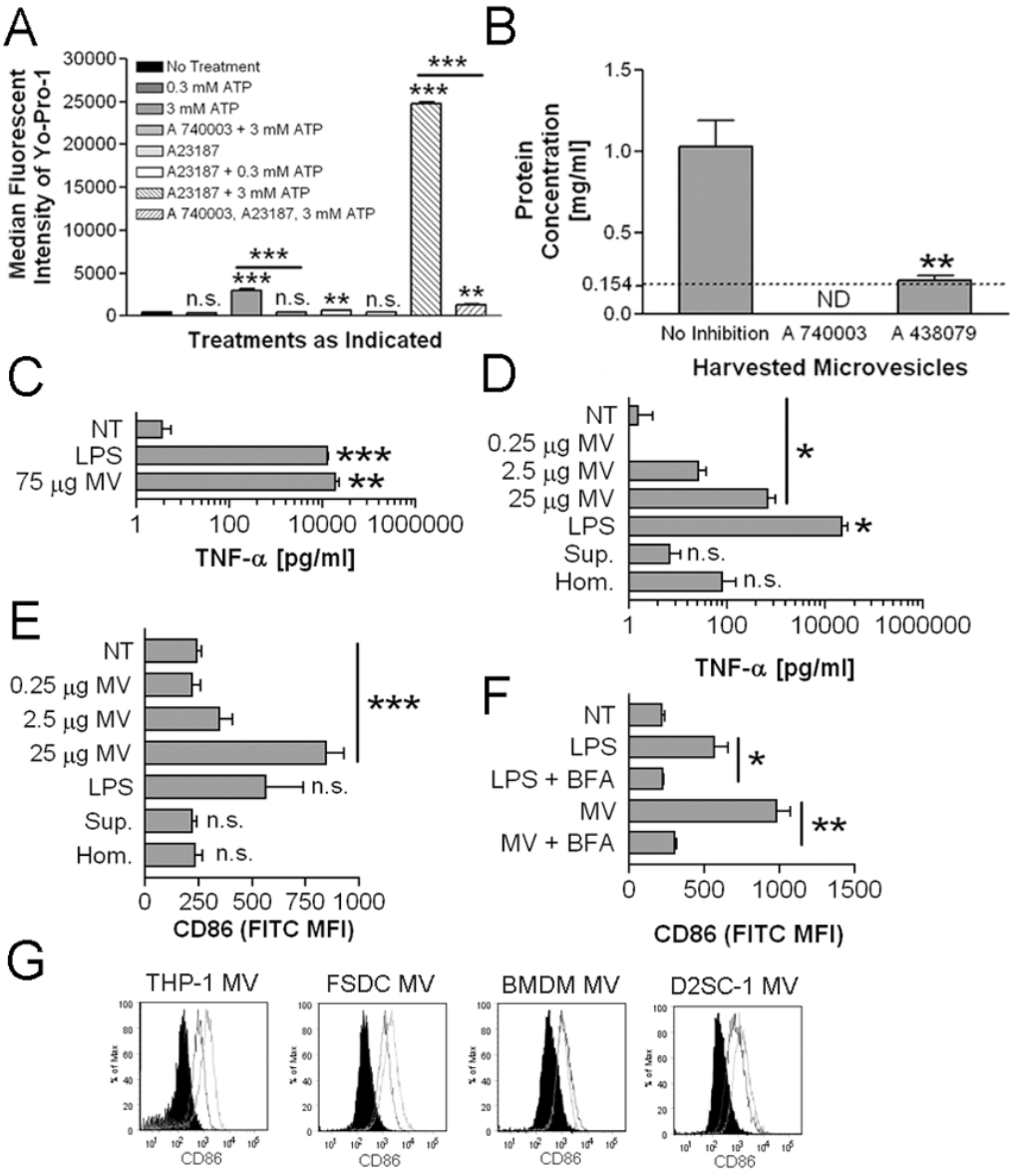

FIGURE 1.

P2X$_7$-induced MV elicit TNF-α secretion and upregulate CD86. *A*, J774A.1 were treated with or without 100 μM A 740003 then given further indicated treatment for 30 minutes. Cells were analyzed for Yo-Pro-1 association by flow cytometry. The histogram indicates median fluorescent intensities means ± SEM of n=3. Statistical comparisons are made to non-treated J774A.1 except where indicated with the inclusion bars. *B*, J774A.1 were treated with or without 100 μM A 740003 or 10 μM A 438079 for 15 minutes prior to MV generation. Harvested MV were quantified for their protein concentration by Bradford Assay. The histogram indicates protein concentration means ± SEM of n=3. Statistical comparisons are made to MV harvested from non-drug treated J774A.1. ND (not detectable) indicates that the protein concentration was lower than the lower limit of detection, which is marked with the dotted line. *C*, BMDM were treated with 1 μg/ml LPS, 75 μg protein equivalents of MV, or were left non-treated for 18 hours. The histogram indicates TNF-α means ± SEM of n=3. The statistical comparison is made to non-treated BMDM. *D*, BMDM were treated with 0.25, 2.5, or 25 μg protein equivalents of MV, 25 μg protein equivalents of

cell homogenate (Hom.), the volume equivalent of 25 μg protein equivalent from ultracentrifugate following generation of MV pellets (Sup.), 1 μg/ml LPS, or were left non-treated for 18 hours. The histogram indicates TNF-α means ± SEM of n=3. The statistical comparison is made to non-treated BMDM. *E*, BMDM from *D* were analyzed for surface CD86 MFI means ± SEM of n=3. The statistical comparison is made to non-treated BMDM. *F*, BMDM were treated with 1 μg/ml LPS, 25 μg protein equivalents of MV, or were left non-treated with or without 10 μg/ml brefeldin A (BFA) for 18 hours. The histogram indicates surface CD86 MFI means ± SEM of n=3. *G*, MV harvested from PMA differentiated THP-1, FSDC, BMDM, or D2SC-1 (25μg protein equivalents) were incubated with 1×10^6 BMDM for 18 hours. CD86 expression induced by MV from each indicated cell (solid line) is compared to CD86 expression induced by an equivalent amount of J774A.1 MV (dotted line) and to non-treated BMDM (black filled). Each flow cytometry histogram is representative of n=2.

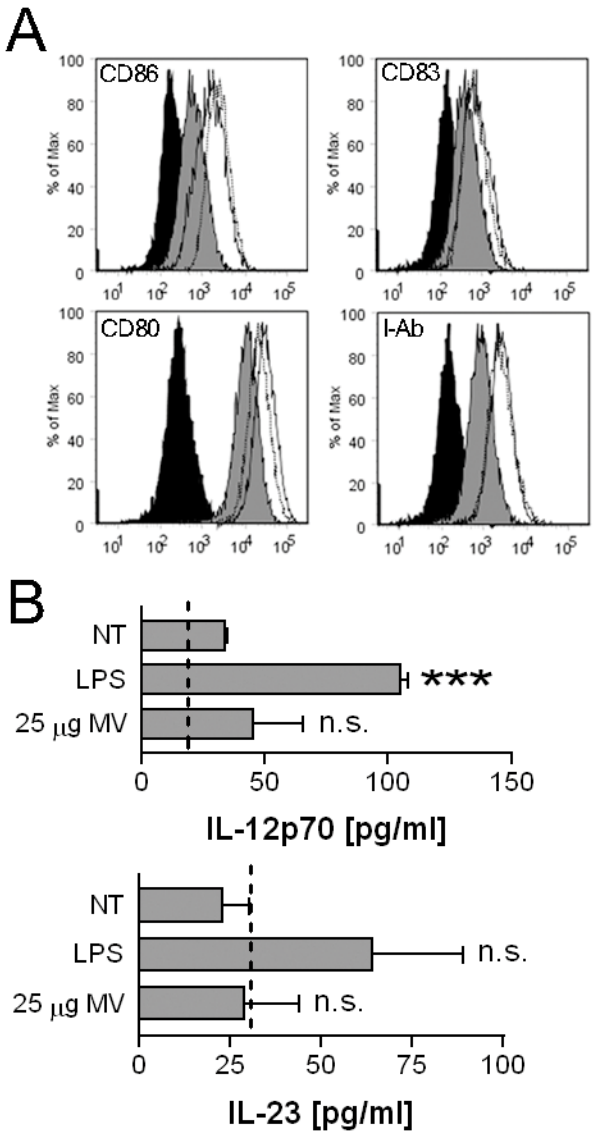

FIGURE 2.

MV upregulate multiple co-stimulatory markers but do not induce IL-12p70 or IL-23 secretion. *A*, BMDM were treated with 1 μg/ml LPS *(solid line)*, 25 μg protein equivalents of MV *(dotted line)*, or were left non-treated *(gray filled)* for 18 hours. Cells were analyzed for CD80, CD83, and CD86 or I-A^b surface expression. Isotype control is shown in *filled in black*. Data is representative of multiple experiments. *B*, BMDM were treated with 1 μg/ml LPS, 25 μg protein equivalents of MV, or were left non-treated for 18 hours. The histogram indicates IL-12p70 or IL-23 means ± SEM of n=3. The statistical comparison is made to non-treated BMDM. The dotted line indicates the bottom limit of detection for each respective ELISA.

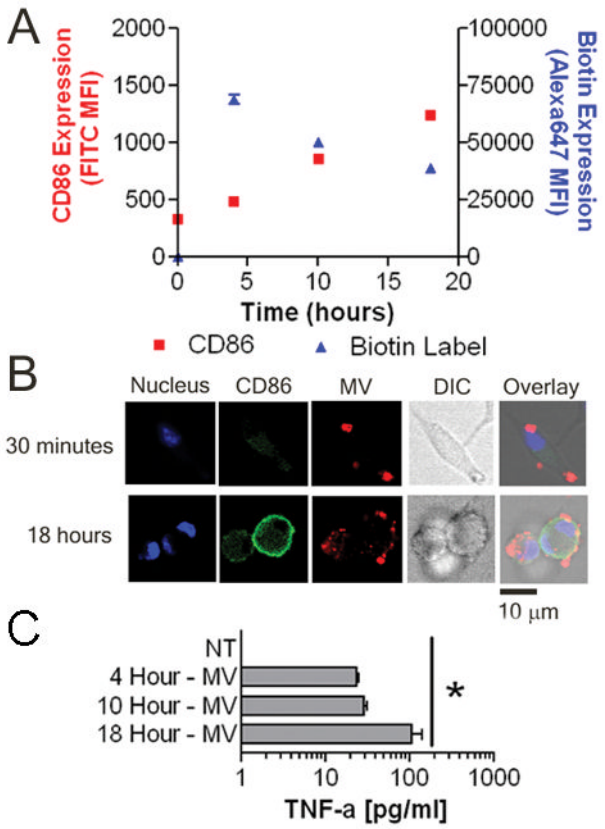

FIGURE 3.

Differential kinetics of TNF-α and CD86 expression relative to surface binding of MV to BMDM. *A*, 5×10^5 BMDM were left untreated or treated with 75 μg protein equivalents of MV for 4, 10, or 18 hours. The histogram indicates means ± SEM of TNF-α released into the supernatant of n=3. *B*, BMDM were left untreated or exposed to 25 μg of biotinylated MV for 4, 10, or 18 hours. Surface CD86 and biotin MFI changes over time are shown. The histogram indicates MFI means ± SEM of n=3. *C*, BMDM were incubated with 25 μg of biotinylated MV for 0.5 or 18 hours. Cells were analyzed for nucleus (*blue*), CD86 (*green*) and biotin (*red*) and expression by confocal microscopy. Differential interference contrast (DIC) image is also shown. Overlay of three fluorescent signals and DIC is shown in the far right image on the panel. Images are representative of 10 random fields of view from two separate experiments. Bar = 10 μm.

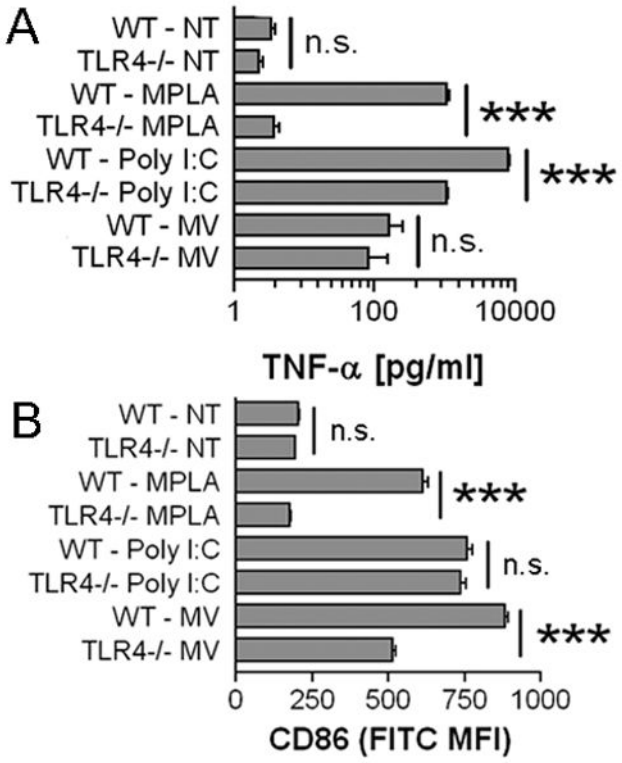

FIGURE 4.

Partial TLR4 dependence of MV-induced BMDM activation. *A*, 5×10^5 WT or TLR4−/− BMDM were treated with 10 μg/ml Poly I:C, 5 μg/ml MPLA, 75 μg protein equivalents of MV, or were left untreated for 18 hours. The histogram indicates TNF-α means ± SEM of n=3. *B*, WT or TLR4−/− BMDM were treated with 10 μg/ml Poly I:C, 5 μg/ml MPLA, 25 μg protein equivalents of MV, or were left untreated for 18 hours. Surface CD86 MFI means ± SEM of n=3 are shown.

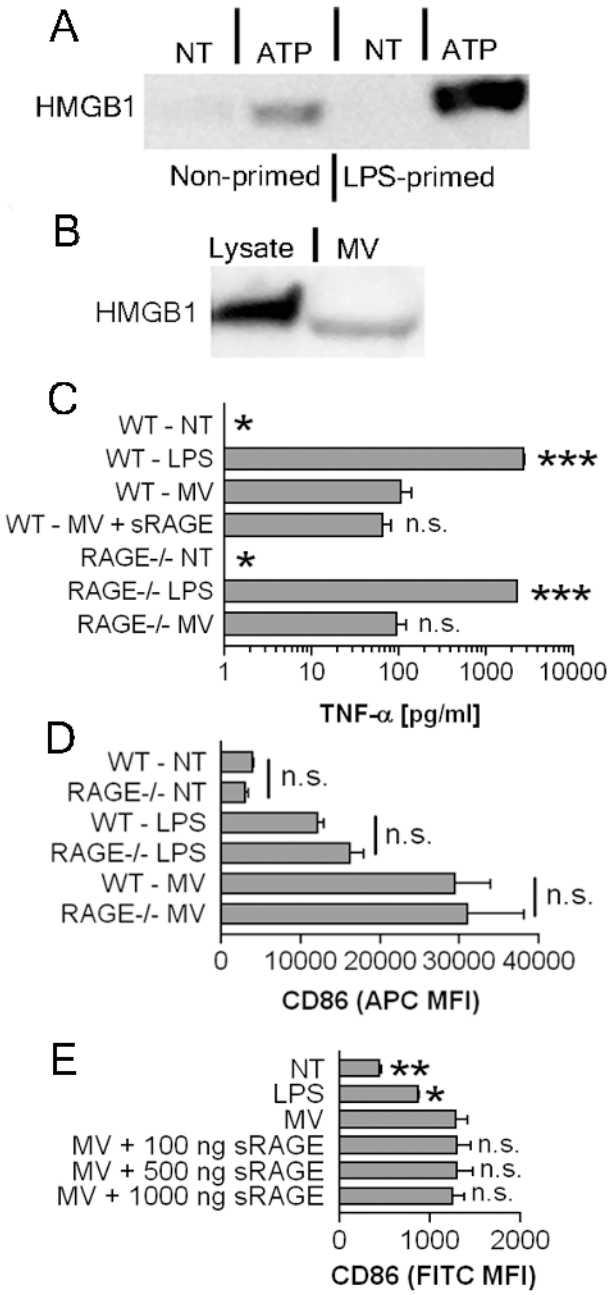

FIGURE 5.

MV contain HMGB1 but CD86 upregulation is HMGB1 independent. *A*, J774A.1 cells were primed with 1 μg/ml LPS or left unprimed for 4 hours, then were treated with 3 mM ATP and 10 μM A23187 for 30 minutes or left untreated. Supernatants were collected, concentrated, and analyzed for HMGB1 by Western blot. Data shown is representative of repeat experiments. *B*, 25 μg protein equivalents from a reference lysate or 25 μg protein equivalents of MV were compared for HMGB1 expression via Western blot. *C*, 5×10^5 WT or RAGE−/−BMDM were treated with 1 μg/ml LPS, 75 μg protein equivalents of MV with or without 30 minute pre-incubation with 1 μg/ml of soluble RAGE, or were left non-treated for 18 hours. The histogram indicates TNF-α means ± SEM of n=3. Statistical comparison is made to WT BMDM treated with 25 μg MV. *D*, WT or RAGE−/− BMDM were treated

with 1 μg/ml LPS, 25 μg protein equivalents of MV, or were left untreated for 18 hours. The histogram indicates surface CD86 MFI means ± SEM of n=3. *E*, 25 μg protein equivalents of MV were pretreated with 100 ng/ml, 500 ng/ml, or 1,000 ng/ml of soluble RAGE for 30 minutes prior to addition to BMDM. No treatment, LPS, and 25 μg protein equivalents of MV were included as controls. Surface CD86 MFI and ± SEM of n=3 are shown. The statistical comparison is made to 25 μg MV alone treated BMDM.

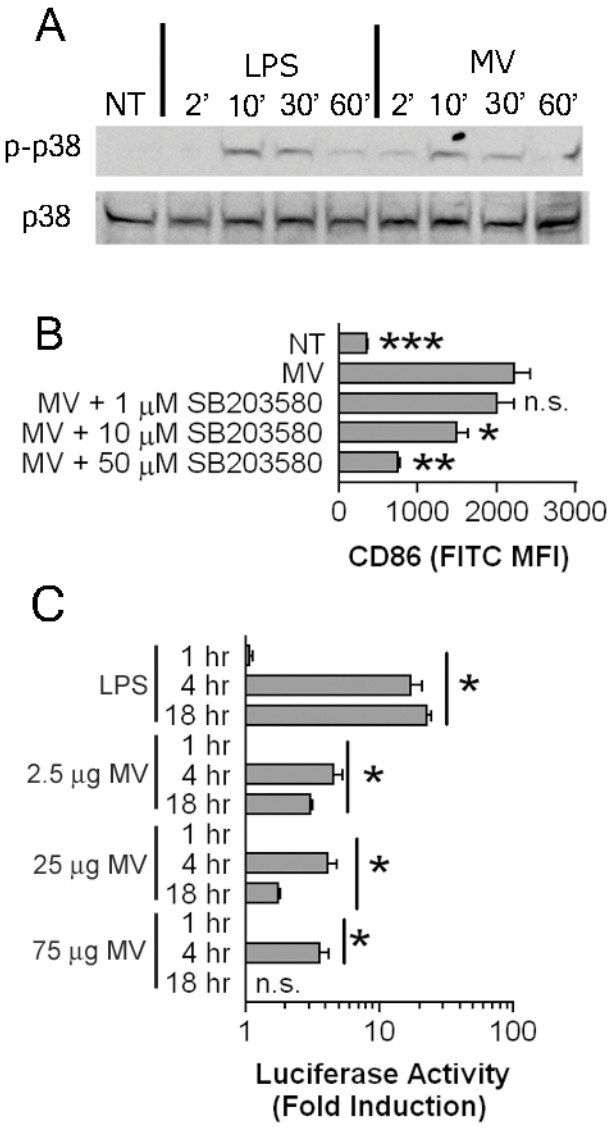

FIGURE 6.

MV activate p38 MAPK and NF-κB pathways. *A*, BMDM were left non-treated or were treated with 1 μg/ml LPS or 25 μg protein equivalents of MV for 2, 10, 30, or 60 minutes. Expression of phosphorylated p38 (p-p38) and total p38 (p38) was evaluated via Western blot. Data is representative of repeat experiments. *B*, BMDM were treated with 25 μg protein equivalents of MV with or without additional treatment of the phosphorylated p38 inhibitor SB203580 at either 1 μM, 10 μM, or 50 μM, or were left non-treated for 18 hours. The histogram indicates surface CD86 MFI means and ± SEM of n=3. The statistical comparison is made to 25 μg MV alone treated BMDM. *C*, RAW264.7 macrophages expressing luciferase under control of an NF-κB promoter were treated with 1 μg/ml LPS, 2.5, 25, or 75 μg protein equivalents of MV for 1, 4, or 18 hours. The fold change over non-treated cells is shown. The histogram indicates fold change means ± SEM of n=3. The statistical comparison is made to the 1 hour fold change value for each respective treatment.

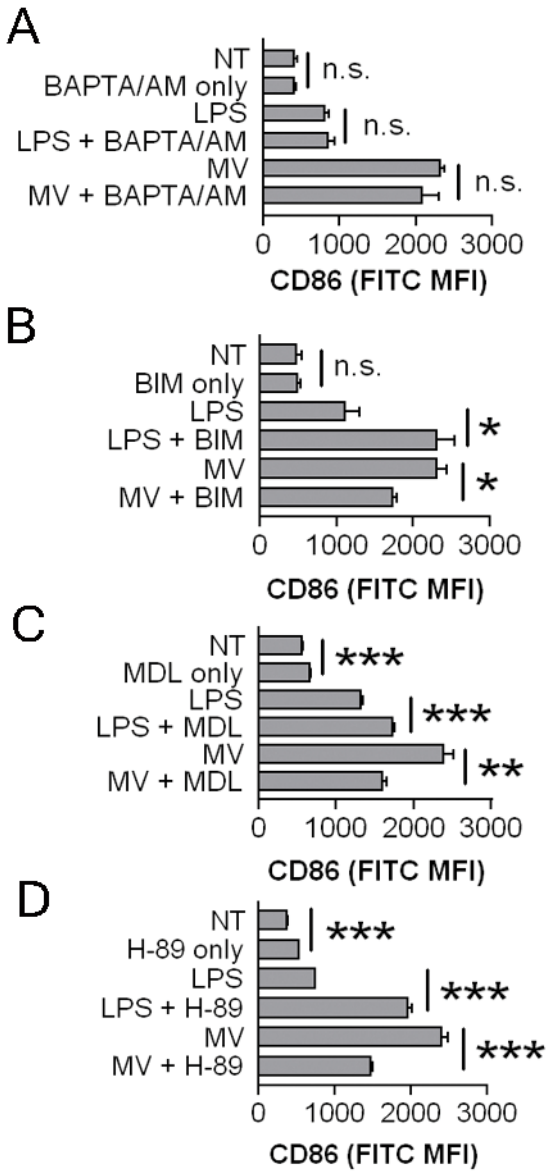

FIGURE 7.

CD86 upregulation is cAMP, PKA, and PKC-dependent, but Ca^{2+}-independent. BMDM were left non-treated or treated with 1 μg/ml LPS or 25 μg of MV with or without additional treatment of 10 μM intracellular calcium chelator BAPTA/AM in *A*, 50 μM PKC inhibitor Bisindolylmaleimide I HCl (BIM) in *B*, 10 μM adenylate cyclase inhibitor MDL-12330A in *C*, or 10 μM PKA inhibitor H-89 in *D*, for 18 hours. Surface CD86 MFI ± SEM of n=3 are shown.

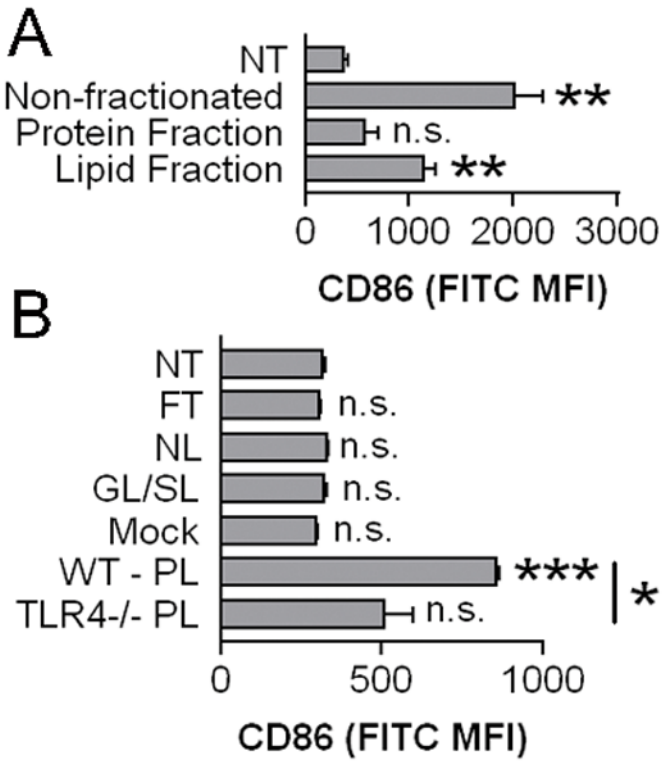

FIGURE 8.

The phospholipid but not protein fraction from MV activates BMDM. *A*, Lipids and protein were isolated from 25 μg protein equivalents of MV and were applied to BMDM for 18 hours. No treatment and non-fractionated 25 μg protein equivalents of MV were included as controls. Surface CD86 MFI means ± SEM of n=3 are shown. The statistical comparison is made to non-treated BMDM. *B*, Total lipid fractions from 225 μg of protein equivalents of MV were isolated and were further fractionated as follows: column flow through (FT), neutral lipids (NL), glycolipids and sulpholipids (GL/SL), and phospholipids (PL). Mock methanol elution of the column without any loaded material was included as a control. Fractions were incubated with BMDM for 18 hours. Non-treated BMDM (NT) and incubation of the phospholipid fraction with TLR4−/− BMDM are also shown. Surface CD86 MFI means ± SEM of n=3 are shown. The statistical comparison is made to non-treated BMDM except where indicated.

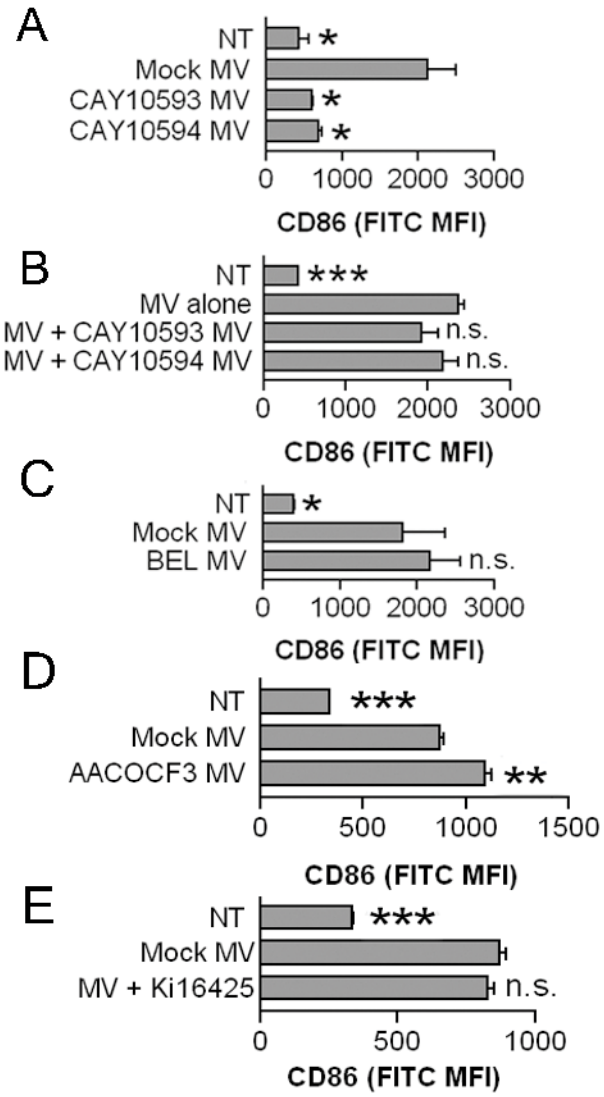

FIGURE 9.

Activities of lipid modifying enzymes PLD1 and PLD2 but not $iPLA_2$ or $cPLA_2$ are required for generating stimulatory MV that can induce CD86 expression. J774A.1 were pretreated with 50 μM PLD1 inhibitor CAY10593 or 50 μM PLD2 inhibitor CAY10594 in *A* and *B*, 10 μM $iPLA_2$ inhibitor bromoenol lactone (BEL) in *C*, 10 μM AACOF3 in *D*, or DMSO vehicle control for 30 minutes prior to and during MV generation. Twenty-five μg of protein equivalents from the generated MV were incubated with BMDM for 18 hours. In *B*, 25 μg of protein equivalents from MV from mock treated J774A.1 were incubated with or without 25 μg of protein equivalents from MV from PLD1 or PLD2 inhibited J774A.1. *E*. BMDM were treated with or without 10 μM Ki16425 prior to MV treatment. Non-treated BMDM are included as controls. Surface CD86 MFI means ± SEM of n=3 are shown. The statistical comparison is made to mock MV treated BMDM.